# *pho2*, a Phosphate Overaccumulator, Is Caused by a Nonsense Mutation in a MicroRNA399 Target Gene[1][W]

**Kyaw Aung[2], Shu-I Lin[2], Chia-Chune Wu, Yu-Ting Huang, Chun-lin Su[3], and Tzyy-Jen Chiou***

Institute of BioAgricultural Sciences (K.A., S.-I.L., C.-C.W., Y.-T.H., C.-l.S., T.-J.C.), and Molecular and Biological Agricultural Sciences Program, Taiwan International Graduate Program (K.A., T.-J.C.), Academia Sinica, Taipei 115, Taiwan, Republic of China; Department of Life Science, National Chung-Hsing University, Taichung 402, Taiwan, Republic of China (K.A., T.-J.C.); and Graduate Institute of Life Sciences, National Defense Medical Center, Taipei 114, Taiwan, Republic of China (S.-I.L., T.-J.C.)

We recently demonstrated that microRNA399 (miR399) controls inorganic phosphate (Pi) homeostasis by regulating the expression of *UBC24* encoding a ubiquitin-conjugating E2 enzyme in Arabidopsis (*Arabidopsis thaliana*). Transgenic plants overexpressing miR399 accumulated excessive Pi in the shoots and displayed Pi toxic symptoms. In this study, we revealed that a previously identified Pi overaccumulator, *pho2*, is caused by a single nucleotide mutation resulting in early termination within the *UBC24* gene. The level of full-length *UBC24* mRNA was reduced and no UBC24 protein was detected in the *pho2* mutant, whereas up-regulation of miR399 by Pi deficiency was not affected. Several characteristics of Pi toxicity in the *pho2* mutant were similar to those in the miR399-overexpressing and *UBC24* T-DNA knockout plants: both Pi uptake and translocation of Pi from roots to shoots increased and Pi remobilization within leaves was impaired. These phenotypes of the *pho2* mutation could be rescued by introduction of a wild-type copy of *UBC24*. Kinetic analyses revealed that greater Pi uptake in the *pho2* and miR399-overexpressing plants is due to increased $V_{max}$. The transcript level of most *PHT1* Pi transporter genes was not significantly altered, except *PHT1;8* whose expression was enhanced in Pi-sufficient roots of *pho2* and miR399-overexpressing compared with wild-type plants. In addition, changes in the expression of several organelle-specific Pi transporters were noticed, which may be associated with the redistribution of intracellular Pi under excess Pi. Furthermore, miR399 and UBC24 were colocalized in the vascular cylinder. This observation not only provides important insight into the interaction between miR399 and *UBC24* mRNA, but also supports their systemic function in Pi translocation and remobilization.

In addition to assimilating carbohydrates in photosynthetic tissues, plants have to acquire mineral nutrients from soil to build up basic components and maintain functional machinery to support their normal growth, development, and reproduction. Among these essential mineral nutrients, phosphorus (P) is one of the least available nutrients in soil. Although the total P content in soil is high, most of it is unavailable for uptake. Concentration of the available P source, inorganic phosphate or orthophosphate (Pi), in the soil solution is usually below that of many other micronutrients (Barber et al., 1963) and seldom exceeds 10 $\mu$M (Bieleski, 1973). The low availability of Pi in the soil solution is mainly caused by the rapid adsorption of Pi to clay and organic substances, precipitation of Pi with cations, or conversion of Pi into organic forms by soil microbes (Marschner, 1995; Holford, 1997; Raghothama, 1999). To reduce Pi deficiency to ensure crop productivity and the impact on the environment because of overfertilization, development of crops with improved Pi acquisition has been a focus of research. To achieve this goal, understanding the physiological, biochemical, and molecular changes under Pi deficiency in regulating Pi homeostasis within plants is necessary.

Plants have developed a series of adaptive responses to enhance Pi acquisition under Pi-limited conditions. These responses include changes in root morphology and architecture, increased Pi uptake activity, secretion of organic acids or phosphatase, and association with mycorrhizal fungi (for review, see Harrison, 1999; Raghothama, 1999; Poirier and Bucher, 2002; Lopez-Bucio et al., 2003; Ticconi and Abel, 2004). Moreover, conservation and remobilization of internal P is also crucial for maintenance of Pi homeostasis within plants. In the recent decade, both genetic and molecular approaches have been used to explore the genes involved in these adaptive responses. With the advantage of genomics tools, a large number of Pi-responsive genes involved in various physiological functions and metabolic pathways have been reported

[1] This work was supported by Academia Sinica (grant no. AS91IBAS2PP) and the National Science Council of the Republic of China (grant no. NSC94–2311–B–001–057) to T.-J.C.

[2] These authors contributed equally to the paper.

[3] Present address: Vita Genomics, Inc., Taipei 248, Taiwan, Republic of China.

* Corresponding author; e-mail tjchiou@gate.sinica.edu.tw; fax 886–2–26515600.

The author responsible for distribution of materials integral to the findings presented in this article in accordance with the policy described in the Instructions for Authors (www.plantphysiol.org) is: Tzyy-Jen Chiou (tjchiou@gate.sinica.edu.tw).

[W] The online version of this article contains Web-only data.

Article, publication date, and citation information can be found at www.plantphysiol.org/cgi/doi/10.1104/pp.106.078063.

(Hammond et al., 2003; Wasaki et al., 2003; Wu et al., 2003; Misson et al., 2005), which is consistent with the roles of Pi involved in different aspects of plant growth and development. Among them, specific genes involved in phospholipid degradation, galactolipid and sulfolipid synthesis, and anthocyanin pathways during Pi deficiency were identified (Misson et al., 2005).

In addition, forward and reverse genetics approaches have identified several Arabidopsis (*Arabidopsis thaliana*) mutants with changes in internal Pi concentration (Poirier et al., 1991; Delhaize and Randall, 1995), Pi uptake (Misson et al., 2004; Shin et al., 2004), root morphology (Li et al., 2006; Sánchez-Calderón et al., 2006), or altered responses under Pi-deficient conditions (Chen et al., 2000; Zakhleniuk et al., 2001; Ticconi et al., 2004; Tomscha et al., 2004; Lopez-Bucio et al., 2005). From a reporter system driven by a Pi starvation-induced promoter, PHOSPHATE STARVATION RESPONSIVE 1 (*PHR1*), encoding a MYB transcription factor, was identified to up-regulate a specific group of Pi-responsive genes through the GNATATNC cis-element (Rubio et al., 2001; Franco-Zorrilla et al., 2004). Interestingly, characterization of a SUMO E3 ligase mutant, *siz1*, suggested that sumoylation is involved in modification of PHR1 function (Miura et al., 2005). A mutant defective in plasma membrane targeting of a Pi transporter (PHT1;1) was recently identified and revealed that the PHOSPHATE TRANSPORTER TRAFFIC FACILITATOR 1 (PHF1) protein mediates this process (González et al., 2005). Furthermore, cross-talk of Pi signaling pathways with the cytokinin and sugar-sensing pathways was proposed by the analyses of several other mutants (Franco-Zorrilla et al., 2002, 2005).

By screening the Pi content of shoots, two Arabidopsis mutants, *pho1* and *pho2*, defective in Pi homeostasis, were identified (Poirier et al., 1991; Delhaize and Randall, 1995). Shoots of the *pho1* mutant displayed a Pi-starvation phenotype because loading Pi into the xylem was impaired (Poirier et al., 1991). In contrast, the shoots of the *pho2* mutant accumulated excessive amounts of Pi and exhibited Pi toxic symptoms because of increased Pi uptake and translocation of Pi from roots to shoots (Delhaize and Randall, 1995; Dong et al., 1998). Nevertheless, normal Pi concentration was maintained in the roots of the *pho1* and *pho2* mutants. *pho1* was shown to be epistatic to *pho2* because the double mutation displayed the *pho1* phenotype (Delhaize and Randall, 1995). Consistent with its role in xylem loading, *PHO1* was later identified to encode a membrane protein located in the stellar cells of the root (Hamburger et al., 2002). However, the *PHO2* gene has not been reported but is suspected to be involved in phloem transport of Pi between shoots and roots or in regulating leaf Pi concentration (Dong et al., 1998).

Recently, we reported that microRNA399 (miR399) controls Pi homeostasis by regulating the expression of a ubiquitin-conjugating E2 enzyme (assigned as UBC24; Kraft et al., 2005) in Arabidopsis (Chiou et al., 2006). Accumulation of *UBC24* mRNA was suppressed by the targeting of miR399, whose expression is up-regulated by Pi starvation (Fujii et al., 2005; Chiou et al., 2006). Significantly, overexpression of miR399 or loss of function of the *UBC24* gene led to accumulation of high Pi content to a toxic level in leaves, which resulted from increased uptake of Pi from roots, increased translocation of Pi from roots to shoots, and retention of Pi in the leaves (Chiou et al., 2006). Moreover, impairment of Pi remobilization from old to young leaves accelerates toxicity in old leaves (Chiou et al., 2006). These observations suggest that interaction between miR399 and *UBC24* regulates Pi homeostasis at the systemic level through long-distance communication.

It is interesting to note that the *pho2* mutant, miR399-overexpressing, and *UBC24* loss-of-function plants all displayed similar phenotypes, except that the defect in Pi remobilization within leaves has not been described in *pho2*. Moreover, *PHO2* was mapped to chromosome 2 (Delhaize and Randall, 1995) near *UBC24*. In this study, we systematically compared the phenotypes of *pho2*, miR399-overexpressing, and *UBC24* loss-of-function plants and demonstrated that *PHO2* is indeed the *UBC24*.

## RESULTS

### *pho2* Mutant Plants Resemble miR399-Overexpressing and *UBC24* Loss-of-Function Plants

The *pho2* mutant was obtained from an ethyl methylsulfonate mutagenesis pool as a Pi overaccumulator (Delhaize and Randall, 1995). To verify the physiological resemblance, *pho2*, miR399-overexpressing, and *UBC24* T-DNA knockout plants (SAIL_47_E01; designated as *ubc24-1*) were compared. In Pi-sufficient soil, they all displayed the Pi toxic symptom as chlorosis and necrosis in the mature leaves (Fig. 1A). In agreement with this phenotype, the Pi concentration in the shoots of these plants was more than 4-fold that of wild-type plants (Fig. 1B). Moreover, these plants showed increased Pi uptake activity from roots (Fig. 1C) and greater Pi distribution from roots to shoots as compared with wild-type plants (Fig. 1D).

The defect in Pi remobilization from old leaves observed in miR399-overexpressing and *ubc24-1* plants (Chiou et al., 2006) was examined in the *pho2* mutant. The Pi distribution among different leaves was inspected during growth (Fig. 2A). As expected, Pi concentration in leaves of *pho2* plants was higher than that of wild-type plants; however, *pho2* mutant plants and wild-type plants exhibited different Pi distribution patterns. Pi concentration in the old leaves (e.g. cotyledons and the first two leaves) of wild-type plants declined over time, which indicates movement of Pi out of the old leaves. In contrast, Pi concentration increased in the old leaves of *pho2* (Fig. 2A). The pulse-chase experiment further verified the ability of Pi remobilization (Fig. 2B). After 10 d of growth in $^{33}$P-free nutrient solution, $^{33}$P radioactivity was mobilized

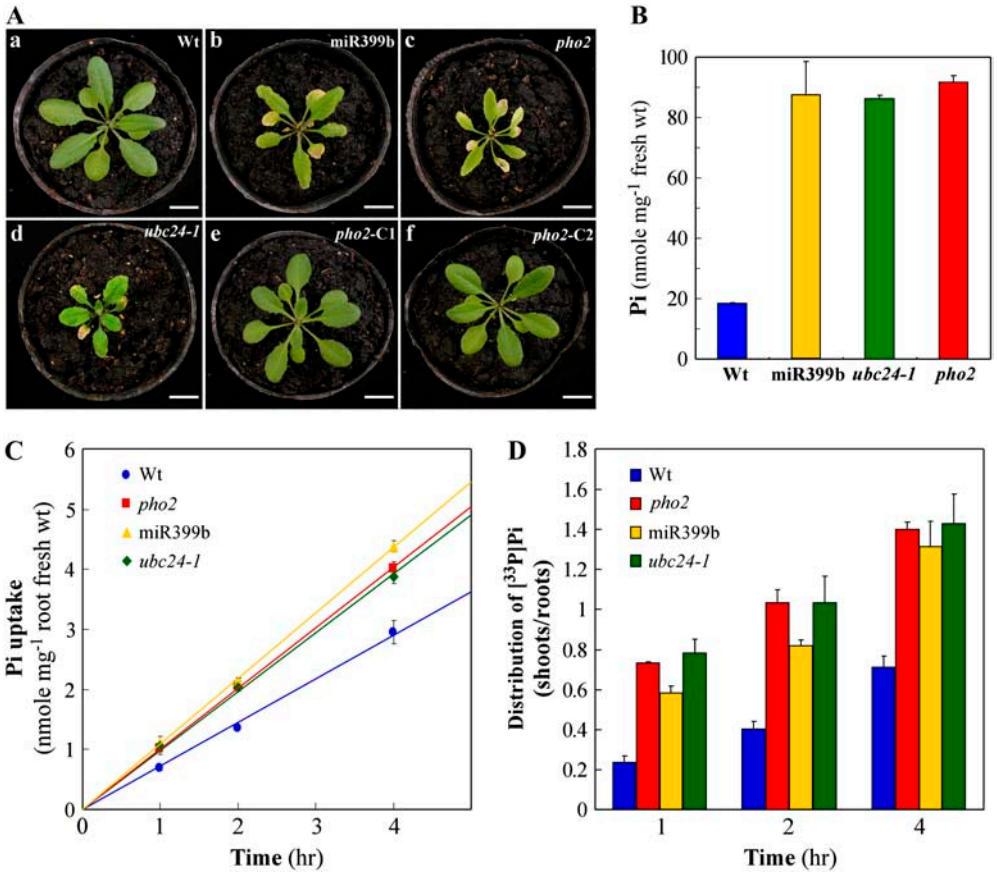


**Figure 1.** Resemblance of Pi toxicity in miR399-overexpressing, *pho2*, and *UBC24* loss-of-function (*ubc24-1*) plants. A, Pi toxic phenotype shown as chlorosis and necrosis in the leaves of 24-d-old miR399b-overexpressing (b), *pho2* (c), and *ubc24-1* (d) plants. Pi toxicity of *pho2* was rescued by transforming a genomic copy of wild-type *UBC24*. Two independent rescued lines, *pho2*-C1 (e) and *pho2*-C2 (f), are shown (see also Fig. 4). a, Wild-type plant. Bar = 1 cm. B, Pi concentration in the shoots of wild-type (Wt; blue), miR399b-overexpressing (miR399b; yellow), *ubc24-1* (green), and *pho2* (red) plants from A. Error bars indicate the SD ($n = 3$). C, Pi uptake activity of wild-type (Wt; blue circles), miR399b-overexpressing (miR399b; yellow triangles), *ubc24-1* (green diamonds), and *pho2* (red squares) plants. Error bars represent the SD ($n = 3$). D, Shoot-to-root ratios of the [$^{33}$P]Pi taken up by wild-type (Wt; blue bars), miR399b-overexpressing (miR399b; yellow bars), *ubc24-1* (green bars), and *pho2* (red bars) plants from C.

out of the old leaves and distributed into the newly developed leaves in wild-type plants, but remained in the old leaves of *pho2* and miR399-overexpressing plants (Fig. 2B). Retention of $^{33}$P radioactivity in these old leaves was associated with the emergence of Pi toxic symptoms (Fig. 2B, asterisks). These data indicate that, like miR399-overexpressing plants, *pho2* mutant plants are also defective in remobilization of Pi out of the old leaves. Taken together, these data show that *pho2*, miR399-overexpressing, and *ubc24-1* plants all show Pi overaccumulation resulting from increased Pi uptake from roots and Pi translocation to shoots, retention of Pi in the leaves, and impaired Pi remobilization within the leaves.

### *pho2* Is Mutated in *UBC24*, a miR399 Target Gene

Initial mapping of *pho2* suggested that the *pho2* locus was linked to the *as1* marker on chromosome 2 (Delhaize and Randall, 1995). The *as1* marker (At2g37630) is close to *UBC24* (At2g33770), about 1.5 Mb apart. cDNA and genomic fragments of *UBC24* in *pho2* were sequenced and a single nucleotide mutation from G to A, causing early termination in the 671 amino acid, was found (Fig. 3A). The termination is located in exon 6 at the beginning of the UBC domain, which suggests loss of ubiquitin conjugation activity of UBC24 in *pho2*.

Expression of *UBC24* and miR399 in *pho2* was further investigated by RNA gel-blot analysis. Content of *UBC24* mRNA was reduced in both roots and shoots of *pho2*, especially under Pi-sufficient conditions (Fig. 3B). A decreased amount of *UBC24* mRNA may reflect the instability of mRNA encoding a truncated nonfunctional protein, a phenomenon called nonsense-mediated mRNA decay (Conti and Izaurralde, 2005). miR399 was up-regulated by Pi deficiency and its accumulation in both roots and shoots was not changed in *pho2* (Fig. 3B).

Protein gel-blot analysis using the anti-UBC24 antibody revealed an approximately 100-kD protein in the

Pi-sufficient roots of wild-type plants, but not in those of *pho2*, miR399-overexpressing, or *ubc24-1* plants (Fig. 3C). No corresponding signal was observed when probing with the preimmune antibody (Fig. 3C), which suggests that this antibody is specific to UBC24. Detection of UBC24 in Pi-sufficient but not Pi-deficient roots of wild-type plants is consistent with the expression pattern of *UBC24* mRNA (Fig. 3B; Chiou et al., 2006), which suggests that expression of *UBC24* may be controlled mainly at the transcriptional or posttranscriptional level. Because of the suppression of *UBC24* mRNA by the overexpression of miR399, no UBC24 protein was detected. Furthermore, a truncated UBC24 (approximately 74 kD) undetectable in the *pho2* mutant could be explained by the reduced amount of *UBC24* mRNA and its translational ability or stability of the truncated UBC24.

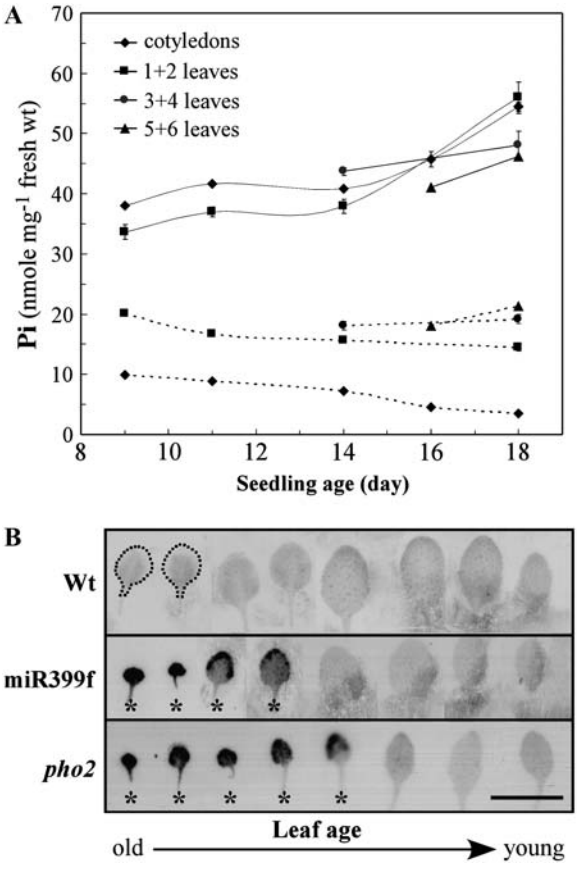


**Figure 2.** Impairment of Pi remobilization in the *pho2* mutant. A, Changes in Pi concentration in the leaves of wild-type plants (dotted lines) or *pho2* mutants (solid lines) grown under Pi-sufficient (1 mM $KH_2PO_4$) conditions. Individual leaves were collected at the indicated times, beginning with 9-d-old seedlings. Leaves from 10 plants were pooled and two proximal leaves were collected as one sample for Pi assay. Error bars represent the SD ($n = 3$). B, Autoradiographs of leaf image obtained from pulse-chase labeling experiments. The first two leaves of wild-type (Wt) plants are outlined because of faint signals. Leaves with chlorosis or necrosis phenotypes in the miR399f-overxpressing (miR399f) and *pho2* plants are marked with asterisks. Bar = 1 cm.

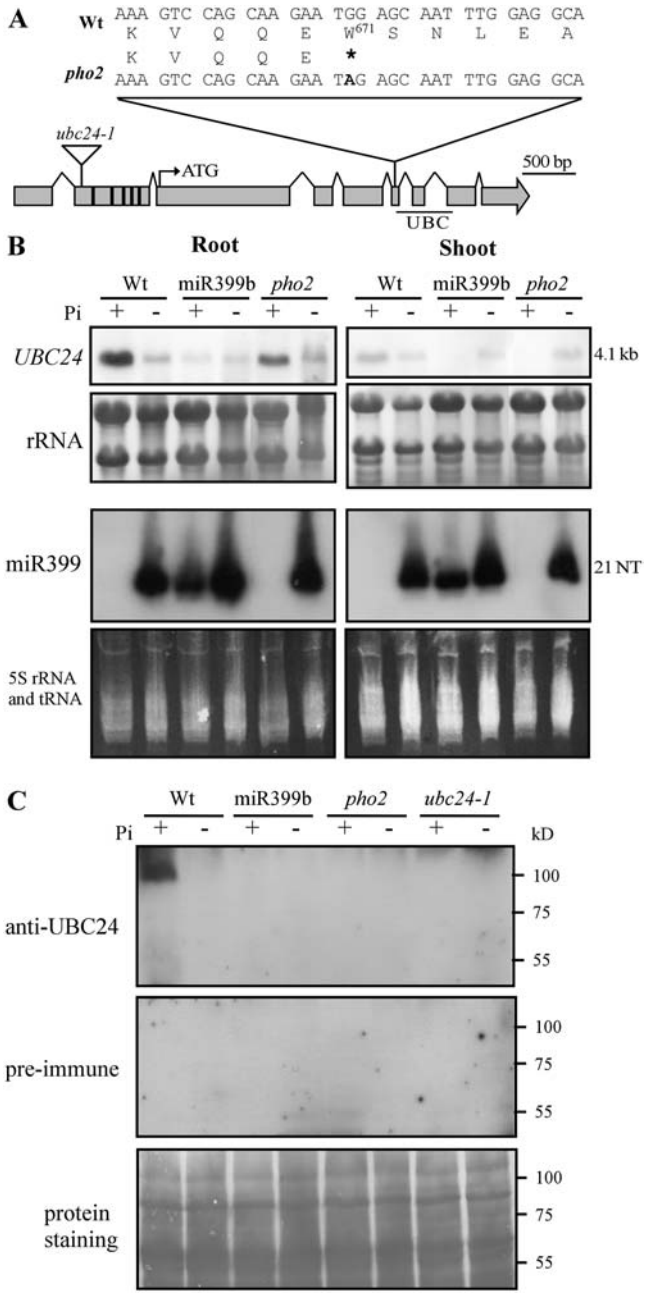


**Figure 3.** A, Mutation of the *UBC24* gene in the *pho2* mutant. An early termination (indicated as the asterisk) at the $W^{671}$ position caused by a single nucleotide change in the sixth exon of *UBC24* was identified in the *pho2* mutant. The translation initiation site and the ubiquitin-conjugating conserved domain (UBC) are indicated. Five miR399 target sequences and the T-DNA insertion in the second exon of the *ubc24-1* mutant are shown. B, RNA gel-blot analyses of *UBC24* (4.1 kb) and miR399 (21 nt) in wild-type (Wt), miR399b-overexpressing (miR399b), and *pho2* plants grown hydroponically under Pi-sufficient (+, 250 $\mu$M $KH_2PO_4$) or Pi-deficient (−) nutrient solution. 5S rRNA and tRNA and 25S and 18S rRNA staining is shown as the loading control. C, Protein gel-blot analysis of the UBC protein in the roots of wild-type (Wt), miR399b-overexpressing (miR399b), *pho2*, and *ubc24-1* plants grown under Pi-sufficient (+) or Pi-deficient (−) media.

To confirm that the *pho2* phenotype is indeed caused by a nonsense mutation in *UBC24*, functional complementation was carried out by introducing a 16.8-kb wild-type genomic copy of *UBC24* into *pho2*. The corresponding entire genomic DNA fragment from the *pho2* mutant was sequenced and showed no other mutation, except the point mutation in the *UBC24* gene. Phenotypes of *pho2* were rescued by wild-type *UBC24*, as observed by lack of Pi toxic symptoms (Fig. 1A), a similar Pi concentration in shoots (Fig. 4A), and distribution of Pi within the leaves to wild-type plants (Fig. 4B). The similarity of *pho2* phenotypes with miR399-overexpressing plants and the *ubc24-1* mutant and the complement of *pho2* phenotypes by *UBC24* strongly demonstrated that the *pho2* locus is *UBC24*.

### Increased Pi Uptake Activity in *pho2* Is a Result of Elevated $V_{max}$

The initial cause for Pi toxicity in *pho2* or miR399-overexpressing plants is the increased uptake of Pi by the root. Because increased Pi uptake activity in *pho2* was more obvious under Pi-sufficient conditions (Dong et al., 1998), plants were grown under 250 $\mu$M $KH_2PO_4$ medium and subjected to kinetic analysis. Pi uptake rate was measured in the uptake solution, with Pi concentrations from 2 to 2,000 $\mu$M. The activities were drawn as Eadie-Hofstee plots (Hofstee, 1952; McPharlin and Bieleski, 1987) to reveal different Pi uptake systems. When the transport activity ($V$) was plotted against $V/[S]$ ($[S]$ is the external Pi concentration in the uptake solution), two distinct lines were derived (Fig. 5A), which suggests two uptake systems with two different affinities (e.g. $K_m$). Interestingly, the $K_m$ for either the low- or high-affinity uptake system in *pho2* and miR399-overexpressing plants was not changed compared with that in wild-type plants. $K_m$ values were 120 to 130 $\mu$M and 10 to 11 $\mu$M for low- and high-affinity uptake systems, respectively (Fig. 5B). However, *pho2* and miR399-overexpressing plants showed higher $V_{max}$ (about 50% increase) than wild-type plants in both uptake systems (Fig. 5B). Thus, we concluded that the increased Pi uptake activity observed in *pho2* (Fig. 1C; Dong et al., 1998) and miR399-overexpressing plants (Chiou et al., 2006) is attributed to elevated $V_{max}$.

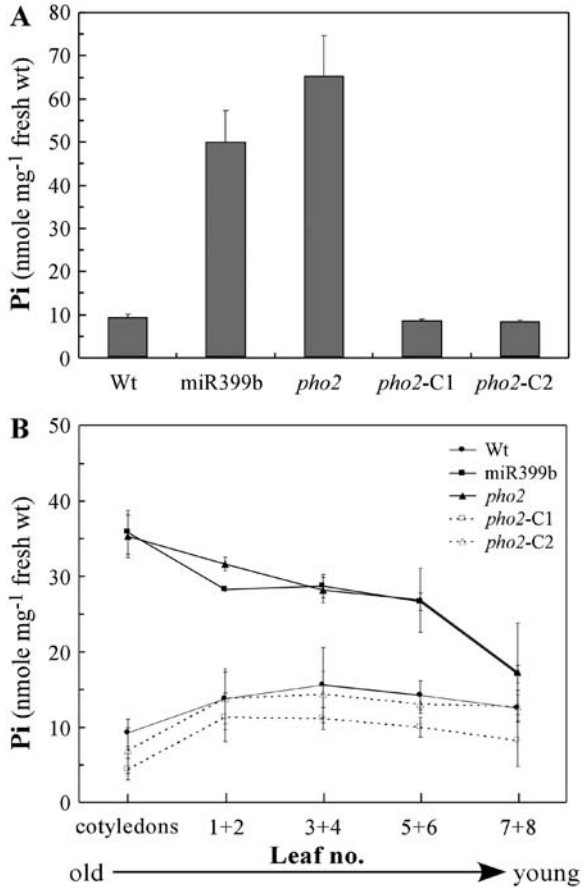


**Figure 4.** Complementation of *pho2* phenotypes by *UBC24*. A, Pi concentration in the shoots of 25-d-old wild-type (Wt), miR399b-overexpressing (miR399b), *pho2*, and two rescued transgenic-line (*pho2*-C1 and *pho2*-C2) plants grown under Pi-sufficient soil. Error bars indicate the SD ($n = 3$). B, Distribution of Pi in the leaves of 19-d-old wild-type (Wt), miR399-overexpressing (miR399b), *pho2*, and two rescued-line (*pho2*-C1 and *pho2*-C2) plants grown under Pi-sufficient (1 mM $KH_2PO_4$) medium. Error bars indicate the SD ($n = 3$).

One possibility for enhanced uptake activity with increased $V_{max}$ without changing $K_m$ is the increase in the molecules of transport proteins. Therefore, we further examined the expression of all members in the Pi transporter (*PHT*) family (Poirier and Bucher, 2002). Root and shoot samples isolated under Pi-sufficient and Pi-deficient conditions were subjected to reverse transcription (RT)-PCR analyses (Fig. 6A). Expression of *PHT1;6*, which is mainly expressed in the anthers (Mudge et al., 2002), was not detected in our samples. Other members of the *PHT1* family were up-regulated by Pi starvation in various degrees in roots and/or shoots, and no differences in expression levels were observed among wild-type, miR399-overexpressing, and *pho2* plants grown under Pi-sufficient or Pi-deficient conditions except for *PHT1;8* (Fig. 6A). Moreover, expression of a plastid Pi transporter, *PHT2;1* (Versaw and Harrison, 2002), and two mitochondrial Pi transporters, *PHT3;2* and *PHT3;3*, was altered in the Pi-sufficient shoots of *pho2* or miR399-overexpressing plants (Fig. 6A). Quantitative PCR was carried out to verify changes in the expression of these Pi transporters (Fig. 6B). Accumulation of *PHT1;8* mRNA was not detected in Pi-sufficient roots of wild-type plants; however, a substantial amount of *PHT1;8* mRNA was detected in Pi-sufficient roots of *pho2* or miR399-overexpressing plants (Fig. 6B). Quantitative PCR experiments also confirmed the down-regulation of *PHT2;1* and the up-regulation of *PHT3;2* and *PHT3;3* in the Pi-sufficient shoots of *pho2* or miR399-overexpressing plants (Fig. 6B). Up-regulation of *PHT3;2* was much greater than that of *PHT3;3*. This observation may be associated with the redistribution of intracellular Pi under excess Pi. Interestingly, induction of *PHT3;2* and *PHT3;3* mRNA by Pi deprivation was reduced in the shoots of *pho2* or miR399-overexpressing

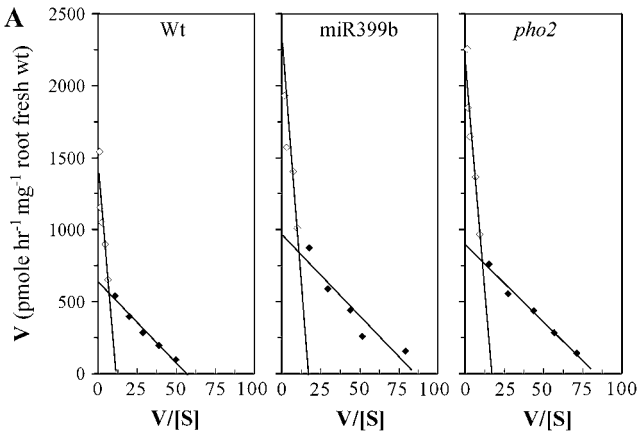


**B**

Kinetic analysis of Pi uptake activity

| | low affinity | | high affinity | |
|---|---|---|---|---|
| | Vmax (pmole $hr^{-1}$ $mg^{-1}$ fw) | Km (uM) | Vmax (pmole $hr^{-1}$ $mg^{-1}$ fw) | Km (uM) |
| **Wt** | 1429±136 | 123±19 | 636±21 | 11.2±0.3 |
| **miR399b** | 2312±97 | 135±24 | 968±1 | 11.3±0.4 |
| ***pho2*** | 2207±31 | 130±4 | 895±59 | 10.7±1.0 |

**Figure 5.** Kinetics analysis of Pi uptake activity. A, Eadie-Hofstee plots of Pi uptake rate for wild-type (Wt), *pho2*, and miR399b-overexpressing (miR399b) plants with 2 to 2,000 $\mu$M Pi concentration. *V* indicates the Pi transport activity and [*S*] the external Pi concentration in the uptake solution. B, $V_{max}$ and $K_m$ values of Pi uptake activity calculated from A. Error bars indicate the SD ($n = 3$).

plants (Fig. 6B), which was not shown by previous RT-PCR analysis (Fig. 6A).

Additionally, we examined the expression of *PHO1*, which is involved in loading Pi into the xylem of roots. No detectable differences in the accumulation of *PHO1* transcripts suggests that *PHO1* may not be associated with increased translocation of Pi from roots to shoots in the miR399-overexpressing or *pho2* mutant plants. However, we did not rule out changes in the protein level of PHO1 in these plants.

### miR399 and UBC24 Are Colocalized in the Vascular Cylinder

The prerequisite for miRNA action is colocalization of miRNA and target transcripts. Although targeting the *UBC24* transcript by miR399 was demonstrated by RACE experiments (Allen et al., 2005), no information was provided for their tissue or cellular locations. Here, the tissue and cellular localization patterns of miR399 and *UBC24* were determined by promoter::reporter analyses. Staining of $\beta$-glucuronidase (GUS) activity driven by the *UBC24* promoter was observed in the vascular tissues of cotyledons, true leaves, and roots (Fig. 7A, a–e). Interestingly, staining was also observed in the vascular tissue of sepals, filaments, anthers, and receptacles (junction between the inflorescence stem and silique; Fig. 7A, f and g). Expression of *UBC24* in the reproductive organs suggests the regulation of Pi transportation by *UBC24* in these organs. Close examination of the GUS signal suggests the localization of UBC24 in the vascular cylinder of the root, including pericycle, vascular tissue, and intervascular regions (Fig. 7A, h).

Consistent with the expression pattern of *UBC24*, *GUS* or green fluorescent protein (*GFP*) expression driven by promoter sequences of miR399a, b, c, d, e, and f genes was also observed in the vascular tissues of roots or leaves subjected to Pi starvation (Fig. 7B, d–q and s), which indicates that these six miR399 genes are all functional and induced by Pi deficiency. Under Pi-sufficient conditions, no reporter signal was detected in most plants (Fig. 7B, a), which suggests that up-regulation of miR399 by Pi deficiency is predominantly contributed by transcriptional regulation. However, weak GUS activity was occasionally detected in the cotyledons of transgenic lines harboring the miR399b or miR399f promoter grown under Pi-sufficient conditions (Fig. 7B, b and c). This observation may reflect the low cloning efficiency of miR399b and miR399f in Pi-sufficient tissues (Sunkar and Zhu, 2004). Reporter activity was not detected in the root tip, except in the miR399b construct (Fig. 7B, h). The GFP or GUS signal in the root driven by other miR399 promoters (Fig. 7B, o and p) or the *UBC24* promoter (Fig. 7A, d) became visible about 250 $\mu$m away from the tip, where the vascular tissue starts to differentiate (Zhu et al., 1998; Stadler et al., 2005). Similar to UBC24, the cross section of root also revealed GUS activity driven by miR399b in the vascular cylinder (Fig. 7B, m). In some cases, the GFP signal driven by miR399f was found specifically in the phloem of roots (Fig. 7B, s). Taken together, these results show that miR399 and UBC24 are colocalized in the vascular cylinder, which further supports their interaction in vivo.

Other than in vascular tissues, GUS or GFP signals were also detected in the mesophyll cells of seedlings driven by miR399e, d, and f promoters (Fig. 7B, j, k, and n; data for expression driven by miR399d not shown), where expression of *UBC24* was not detected. This observation may explain our previous finding that even miR399 was accumulated in both roots and shoots in similar amounts and targeting miR399 to the *UBC24* transcript in the shoots was not as efficient as that in the roots (Chiou et al., 2006). Nevertheless, the function of miR399 in the mesophyll cells remains to be studied.

## DISCUSSION

### *UBC24* Is the *PHO2* Gene

From genetic screening, the *pho2* mutant was identified as a Pi overaccumulator (Delhaize and Randall,

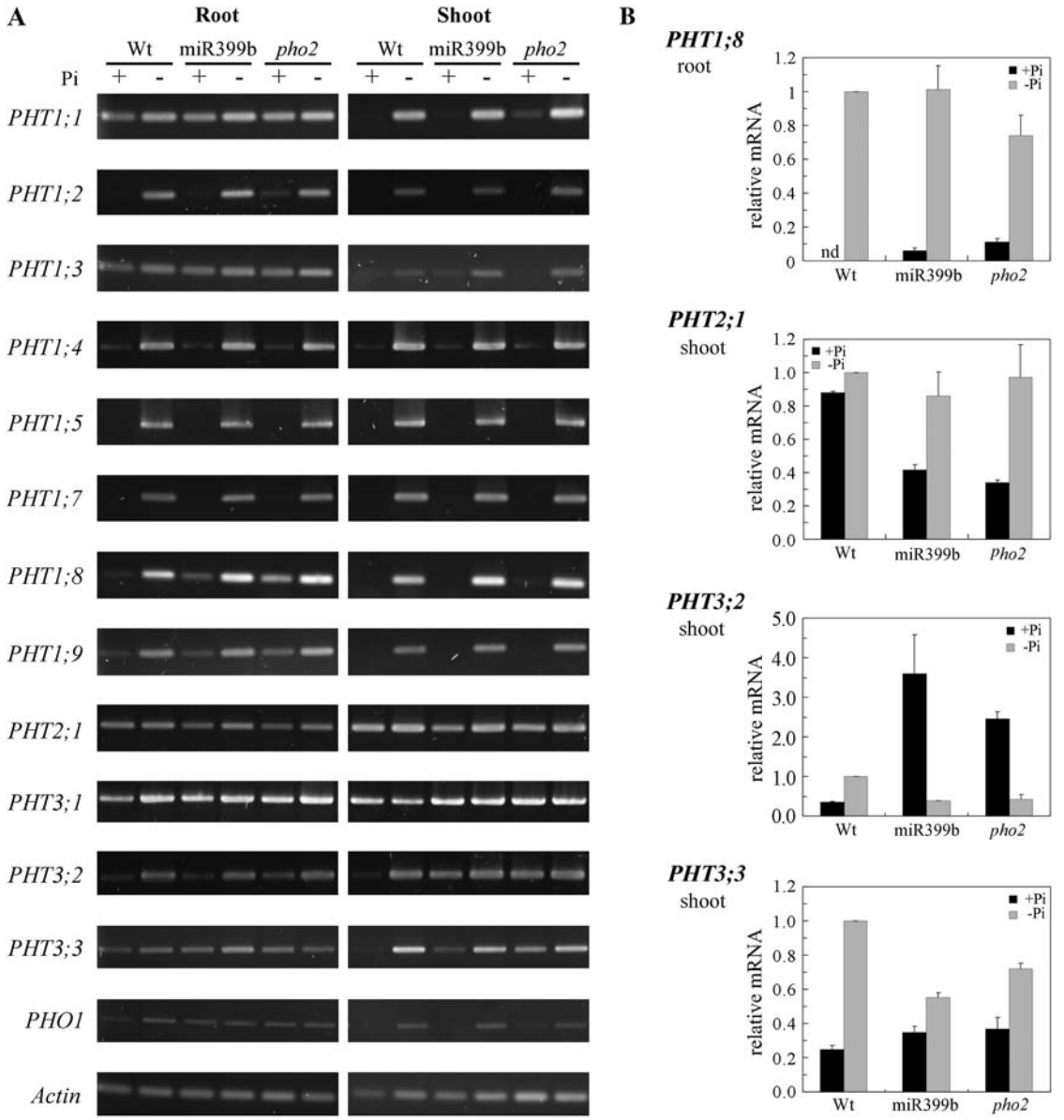


**Figure 6.** Expression of members of *PHT1*, *PHT2*, and *PHT3* families and *PHO1* in wild-type, miR399b-overexpressing, and *pho2* plants. A, RT-PCR analyses of mRNA levels in the root and shoot samples collected from Pi-sufficient (+Pi) or Pi-deficient (−Pi) conditions. B, Quantitative PCR analyses of the relative amount of *PHT1;8*, *PHT2;1*, *PHT3;2*, and *PHT3;3* mRNA. Error bars indicate the SD ($n = 2$). Expression of *PHT1;8* was nondetectable (nd) in the Pi-sufficient roots of wild-type plants.

1995; Dong et al., 1998). Recently, we observed a phenotype similar to *pho2* when miR399 was overexpressed or its target gene, *UBC24*, was knocked out (Chiou et al., 2006). Although remobilization of Pi within the leaves was not previously described in *pho2*, here we showed that *pho2*, miR399-overexpressing, and *ubc24-1* plants all display Pi toxic symptoms (Fig. 1, A and B) as a consequence of enhanced Pi uptake (Fig. 1C), facilitated translocation of Pi from roots to shoots (Fig. 1D), and impaired Pi remobilization from old to young leaves (Fig. 2). Because of these similarities and the initial mapping of *pho2* close to *UBC24*, we reasonably hypothesized that *pho2* could be defective in the expression of *UBC24*. Sequence and expression analyses of *UBC24* in *pho2* (Fig. 3) and complementation of the *pho2* phenotype by the wild-type copy of *UBC24* (Figs. 1A and 4) demonstrated that *UBC24* is the *pho2* gene.

Based on the $^{32}$Pi feeding experiment on a single leaf, Dong et al. (1998) showed that translocation of $^{32}$Pi from shoots to roots was partially defective in *pho2* under both Pi-sufficient and Pi-deficient conditions. *pho2* appeared to retain Pi in shoots because the excess Pi in the shoots of *pho2* was not translocated to roots during Pi deprivation (Dong et al., 1998). These results support our observations concerning the ineffectiveness

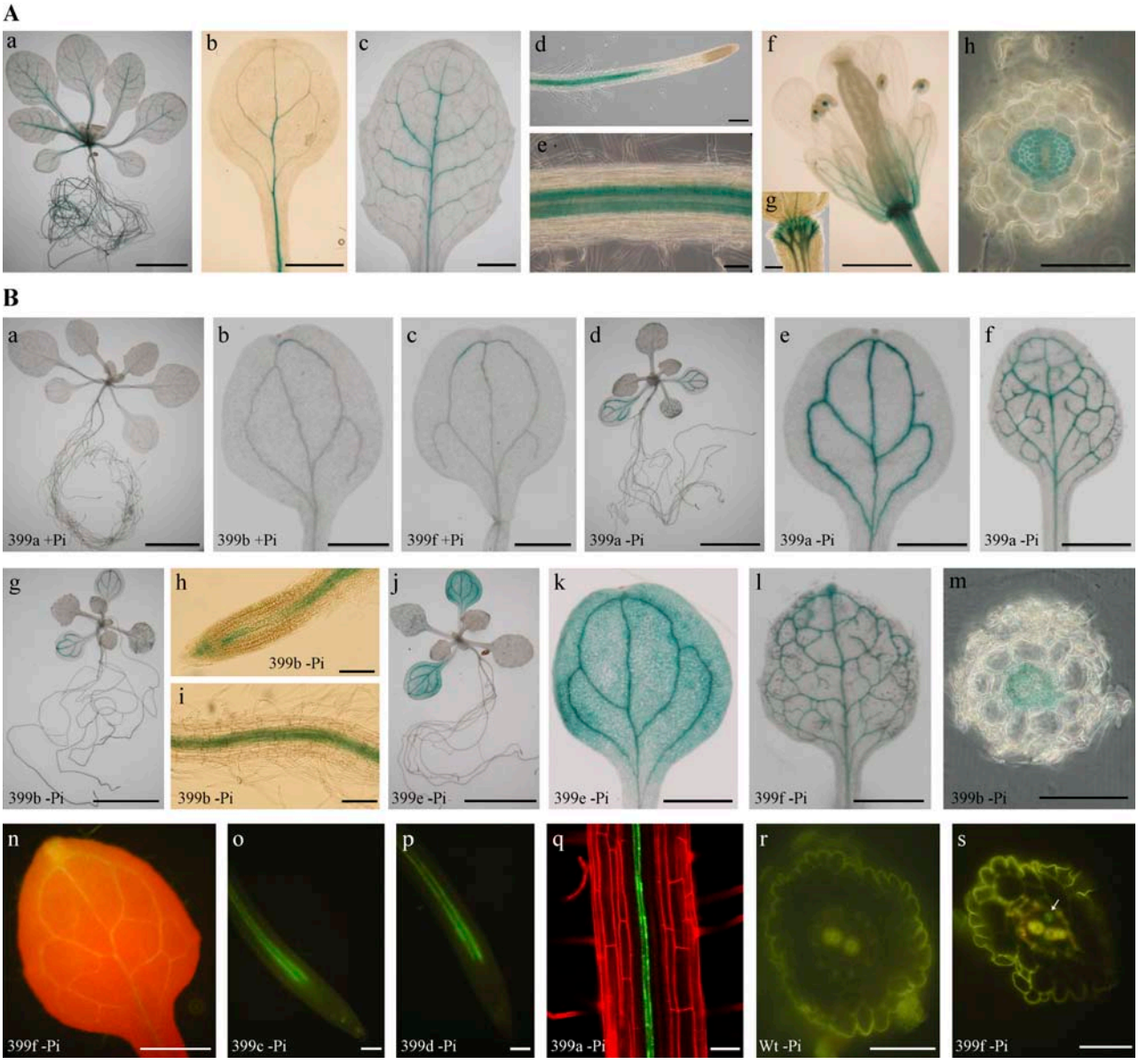


**Figure 7.** Tissue and cellular localization of *UBC24* and miR399 by promoter::reporter analyses. A, GUS staining in the vascular tissues of *UBC24* promoter::GUS transgenic plants grown under Pi-sufficient conditions. a, Whole seedling; b, cotyledon; c, the third true leaf; d and e, root; f, flower; g, enlarged receptacle; h, cross section of the root. The strong signal in the middle of pollen indicates the central vascular tissues. B, GUS staining (a–m) or GFP florescence (n–q and s) in miR399 promoter::reporter transgenic plants. All seedlings were grown under Pi-deficient media (−Pi) except those in a, b, and c, which were grown under Pi-sufficient media (+Pi). The growth condition and expression driven by different miR399 promoters was indicated in each image. a, d, g, and j, Whole seedling; b, c, e, and k, cotyledon; f, l, and n, first true leaf; h, i, o, p, and q, root; m, r, and s, cross section of root. r, Root section from Pi-starved wild-type plants showing autofluorescence in the epidermis and xylem. s, Arrow indicates the GFP signal in the phloem of the root. n, Red is the fluorescence of chlorophyll. q, Red fluorescence of cell walls results from staining with propidium iodide. Bar = 5 mm in A, a; and B, a, d, g, and j. Bar = 1 mm in A, b, c, and f; and B, b, c, e, f, k, l, and n. Bar = 100 $\mu$m in A, d and g; and B, h, i, o, and p. Bar = 50 $\mu$m in A, e and h; and B, m, q, r, and s.

of Pi mobilization out of old leaves of *pho2* or miR399-overexpressing plants (Fig. 2). The opposite result was noted by Delhaize and Randall (1995), who measured Pi concentrations in the fully expanded leaves before and after 4 d of Pi deprivation and found that most of the Pi can be mobilized out of the leaves of *pho2*. We also observed the reduction of Pi concentration in the old leaves of *pho2* or miR399-overexpressing plants under Pi deficiency; however, unlike wild-type plants in which the oldest leaf contained the lowest concentration of Pi, the oldest leaf of *pho2* or miR399-overexpressing plants accumulated Pi at the highest concentration among all leaves (Chiou et al., 2006). Abnormal distribution of Pi in the leaves of *pho2* or

miR399-overexpressing plants implies that translocation of Pi out of the old leaves is not as efficient as wild-type plants even under Pi-deficient conditions. Moreover, we observed that the defect in mobilization of Pi out of the old leaves of *pho2* was less severe when plants were grown under Pi-deficient, rather than Pi-sufficient, conditions (data not shown). Induction of an alternative pathway to enhance Pi remobilization under Pi deprivation is thus necessary to compensate the situation.

### Altered Expression of Specific *PHT* Genes in *pho2*

The dual transport system with low and high affinity for nutrient uptake (Epstein, 1976) has been widely accepted. A single-phase or multiphase Pi transport system has been described in many plant species or cultured cells (Ullrich-Eberius et al., 1984; McPharlin and Bieleski, 1987; Nandi et al., 1987; Mimura et al., 1990; Furihata et al., 1992; Shimogawara and Usuda, 1995; Dunlop et al., 1997; Narang et al., 2000). Our data suggest that Arabidopsis possesses a dual Pi uptake system under the conditions we analyzed: a low-affinity system operating at high Pi concentration ($K_m$ = 120–130 $\mu$M) and a high-affinity system operating at low Pi concentration ($K_m$ = 10–11 $\mu$M; Fig. 5). This finding is different from the previous observation of only one Pi uptake system in Arabidopsis (Narang et al., 2000). We suspect that a narrow Pi concentration range (2.5–100 $\mu$M) in the kinetic assay may overlook this dual-affinity system. With a concentration range from 0.5 $\mu$M to 5 mM, Dunlop et al. (1997) also reported two mechanisms operating Pi uptake in Arabidopsis, which is consistent with our results. The kinetic analysis suggests that increased Pi uptake activity by overexpressing miR399 or loss-of-function *UBC24* is caused by elevated $V_{max}$ in both low- and high-affinity transport systems without alteration of $K_m$ (Fig. 5B). However, we did not observe differences in the value of $V_{max}$ and $K_m$ between wild-type and *pho2* mutant plants grown under Pi-deficient conditions (data not shown). This finding is consistent with a previous report that increased Pi transport activity was not detected in *pho2* under Pi-deficient conditions (Dong et al., 1998).

In our system, the transport activity was conducted in whole seedlings and the $V_{max}$ and $K_m$ were measured as a sum of various transporters, which is much more complicated than the reaction operated by a single protein. We postulate two possibilities for increased $V_{max}$ without a change in substrate affinity: the increased amount of transporter molecules per se and the increased catalytic activity, such as the translocation of substrate across membrane. The up-regulation of *PHT1;8* transcripts in Pi-sufficient roots of miR399-overexpressing and *pho2* plants (Fig. 6) suggests that UBC24 may act upstream of *PHT1;8* to suppress its expression under Pi-sufficient conditions. Because the UBC-E2 enzyme does not normally participate in regulating transcriptional activity, the reduction of *PHT1;8* transcripts by UBC24 may be mediated through an intermediate, possibly a transcription factor that is the target of ubiquitination mediated by UBC24. However, the increased level of *PHT1;8* transcripts in Pi-sufficient roots of *pho2* or miR399-overexpressing plants was only 10% of that induced by Pi deficiency (Fig. 6B). Whether increased expression of *PHT1;8* transcripts is responsible for the increased number of transporter molecules, thus resulting in greater $V_{max}$ (Fig. 5), or enhancing Pi translocation into shoots (Fig. 1D) remains to be investigated. It is intriguing to find out where *PHT1;8* is expressed. Unfortunately, promoter::reporter analysis of *PHT1;8* failed to identify tissue localization (Mudge et al., 2002). Where *PHT1;8* is expressed and how it functions in concert with UBC24 located in the vascular tissue are topics for further study. In addition to expression of *PHT1;8*, that of other intracellular Pi transporter genes, such as *PHT2;1*, *PHT3;2*, and *PHT3;3*, was altered (Fig. 6B). Although efflux or influx of these Pi transporters is not clearly defined yet, changes in their expression indicate the adjustment of Pi partitioning across different organelles when intracellular Pi concentration is too high. Fujii et al. (2005) reported that accumulation of *PHT1;1* mRNA was slightly increased in the miR399-overexpressing plants under Pi-sufficient conditions, but we did not observe this. Differences in plant stages or growth and treatment conditions may not reproduce this marginal change. Consistent with our results, Smith et al. (1997) did not observe differences in the transcript level of *APT1* (*PHT1;2*) and *APT2* (*PHT1;1*) in roots of *pho2* and wild-type plants.

That the transcript level of *PHT1* transporters did not change markedly under Pi-deficient conditions (Fig. 6A) is in agreement with unaffected transport activity (Dong et al., 1998) and could be due to the down-regulation of *UBC24* by Pi deficiency. Although most of the Pi transporters examined did not show changes in their transcript level, it is likely that they are regulated at the posttranslational step via ubiquitination-mediated protein degradation through UBC24. Specific antibodies directed against these Pi transporters are needed to prove this hypothesis. Recently, PHF1 was identified to be required for localization of the PHT1;1 Pi transporter to the plasma membrane (González et al., 2005). It is of interest to know whether enhanced Pi uptake activity in *pho2* or miR399-overexpressing plants is the consequence of enhanced PHF1 activity, resulting in targeting more Pi transporters to the plasma membrane.

### Vascular Localization and Systemic Effects on Whole-Plant Pi Homeostasis

Colocalization of miR399 and UBC24 in the vascular cylinder (Fig. 7) supports targeting *UBC24* mRNA by miR399. *UBC24* is predominantly expressed in vascular tissue, whereas miR399 is also expressed in the root tip and mesophyll cells in addition to vascular tissue (Fig. 7B, h, j, k, and n). However, it does not seem

logical that miR399 is expressed in these cells where its target gene, *UBC24*, is not expressed. We suspect that other unidentified target genes of miR399 may be expressed in these cells or that the expression of miR399 in these cells is just a remnant during evolution.

It is of interest to note that GUS staining driven by the miR399 promoter was initiated in the vascular tissues of leaf tips (Fig. 7B, b and c) and gradually moved toward the base upon Pi starvation (Fig. 7B, g and n). This observation coincides with the trend of leaf maturation and the emergence of chlorosis and necrosis symptoms of Pi toxicity. In contrast to this basipetal expression pattern, GUS staining driven by the *UBC24* promoter was acropetal. The signal was strongly observed at the petiole and leaf base and gradually diffused toward the leaf margins (Fig. 7A, a–c). These opposite expression patterns between miR399 and *UBC24* may be correlated with their antagonistic effects.

The vascular location of miR399 and UBC24 is particularly fascinating because it correlates well with the systemic effects observed in *pho2*, miR399-overexpressing, and *ubc24-1* plants, such as Pi translocation between roots and shoots and Pi mobilization within leaves. Pi uptake by roots might be regulated by Pi recycling in the phloem (Drew and Saker, 1984; Schjørring and Jensén, 1987). Increased Pi uptake and reduced Pi recycling by overexpression of miR399 or loss of function of UBC24, which are all expressed in the vascular tissues, support this hypothesis. Enhanced Pi uptake activity did not occur in the detached *pho2* roots without shoots (Dong et al., 1998), which suggests that a systemic signal derived from the shoot controls the increased uptake of Pi. Moreover, ineffective down-regulation of a Pi starvation-induced gene, *At4*, in *pho1* roots grown under Pi-sufficient conditions, supports translocation of a shoot-derived signal molecule to roots (Burleigh and Harrison, 1999). Transmission of this shoot-derived signal to roots requires passage through the phloem, which may depend on coordination between miR399 and UBC24, also located in the vascular tissues. Further studies focusing on the regulatory pathways of miR399/UBC24 are necessary to uncover this systemic signal molecule.

## MATERIALS AND METHODS

### Plant Materials and Growth Conditions

Arabidopsis (*Arabidopsis thaliana*) wild-type plants (Col 0), miR399-overexpressing (Chiou et al., 2006) and *UBC24* T-DNA knockout plants (*ubc24-1*, SAIL_47_E01), and *pho2* mutant plants (Delhaize and Randall, 1995) requested from the Arabidopsis Biological Resource Center (ABRC) were used for this study. Seeds were surface sterilized and germinated on agar plates with one-half modified Hoagland nutrient solution containing 1 mM $KH_2PO_4$ (sufficient Pi; +Pi), 1% Suc, and 1% Bactoagar. For hydroponic culture, Pi starvation was initiated by transferring 2-week-old seedlings originally grown in high-Pi solution (250 $\mu$M instead of 1 mM $KH_2PO_4$ was used to reduce Pi toxicity) into Pi-free solution. After 11 d, root and shoot samples were collected separately for Pi assay or RNA isolation. For liquid culture, 20-d-old seedlings grown in high-Pi B5 liquid medium were subjected to Pi starvation treatment by transferring them into Pi-free medium for 5 d. Root samples were collected for protein isolation. All growth conditions were at 22°C under a 16-h photoperiod with cool fluorescent light at 100 to 150 $\mu$E $m^{-2}$ $s^{-1}$.

### RNA Gel-Blot and PCR Analyses

RNA isolation and RNA gel-blot analyses were performed as described previously (Lin et al., 2005). Total RNA was treated with DNase I (Ambion) prior to RT-PCR analyses to eliminate genomic DNA contamination. cDNA was synthesized from total RNA by SuperScript III RNase $H^-$ reverse transcriptase (Invitrogen). Quantitative RT-PCR was performed by using the FastStart DNA Master SYBR Green I kit on the LightCycler machine (Roche), following the manufacturer's instructions. The amplification program was performed at 95°C for 10 s, 60°C for 5 s, and 72°C for 10 s. Relative quantitative results were calculated by normalization to *Actin2*. All PCR products were verified by sequencing. PCR conditions and sequences of primers are listed in Supplemental Tables I and II.

### Complementation of the *pho2* Mutant

A 16.8-kb *Kpn*I- and *Nco*I-digested genomic DNA fragment containing the wild-type copy of the *UBC24* gene was isolated from a T1B8 bacterial artificial chromosome clone (requested from the ABRC) and subsequently constructed into the pCAMBIA 1,300 binary vector. DNA was introduced into the *pho2* mutant by the floral-dip method (Clough and Bent, 1998).

### Phosphorous Content Analysis

Pi content was determined as described (Ames, 1966) with minor modifications (Chiou et al., 2006).

### Pi Uptake Analysis and Pulse-Chase Labeling

Twelve-day-old seedlings grown on one-half modified Hoagland medium supplemented with 250 $\mu$M of $KH_2PO_4$ were used for Pi uptake assay. The uptake assay was performed as previously described (Chiou et al., 2006). Kinetic analysis was carried out over a broad range of external Pi concentrations (2, 5, 10, 20, 50, 100, 200, 500, 1,000, and 2,000 $\mu$M $KH_2PO_4$, indicated as substrate concentration [*S*]). To reveal different transport systems, Eadie-Hofstee plots (Hofstee, 1952) were applied whereby the transport activity (*V*) was drawn as the function of $V/[S]$. $K_m$ was calculated from $V = -K_m \times (V/[S]) + V$ and $V = V_{max}$ when $V/[S] = 0$. Pulse-chase labeling was performed as described (Chiou et al., 2006).

### Antibody Production and Protein Gel-Blot Analysis

The recombinant protein corresponding to the 468 to 642 amino acids of UBC24 protein was expressed, purified, and used as an antigen to immunize rabbits. Total proteins of roots from liquid culture were extracted with Tris-HCl buffer (60 mM, pH 8.5) containing 2% SDS, 2.5% glycerol, 0.13 mM EDTA, and 1% protease inhibitor cocktail (Roche). The protein amount was measured by use of DC protein assay reagents (Bio-Rad) with bovine serum albumin as a standard. An amount of 100 $\mu$g of total protein was separated in 10% SDS-PAGE and then transferred to polyvinylidene difluoride membrane (Millipore). The membrane was probed with the preimmune antibody or antibody directed against the UBC24 protein, followed by secondary antibody conjugated with horseradish peroxidase (Pierce). The signal was subsequently detected by use of SuperSignal West Dura Extended Duration substrate (Pierce). Afterward, the membrane was stained with 0.1% (w/v) amido black to ensure a compatible amount of loading.

### Localization of miR399 and *UBC24*

The upstream sequences from the initiation site of *UBC24* and the precursor fold-back structure of six miR399 genes (miR399a, b, c, d, e, and f) were cloned and used to drive expression of *GUS* or *mGFP* reporter genes. The primer sequences and promoter lengths are listed in Supplemental Table III. The 5′-untranslated region of *UBC24*, consisting of the target sequences of miR399, was not included in the *UBC24* promoter construct. These promoter sequences were cloned by PCR, verified by sequencing, and subcloned into pMDC204 (Curtis and Grossniklaus, 2003) to drive expression of an *mGFP*

reporter gene or into pKGWFS7.0 (Karimi et al., 2005) to drive expression of *GUS* reporter genes. These constructs were introduced into Arabidopsis by the floral-dip method (Clough and Bent, 1998). Transgenic T2 plants grown under Pi-sufficient and Pi-deficient conditions underwent reporter analysis. GUS activity was detected according to Lin et al. (2005) and the signal was observed under an Olympus SZX12 or a Zeiss AxioSkop microscope. The GFP signal was observed under a Zeiss AxioSkop fluorescence microscope or a Zeiss LSM 510 Meta confocal microscope.

## ACKNOWLEDGMENTS

We thank Dr. Kuo-Chen Yeh and Dr. Yee-Yung Charng for critically reading the manuscript. We also thank Wen-Chien Lu, Su-Fen Chiang, and Ya-Ni Chen for technical assistance, and Hsing-Yu Huang for plant propagation.

Received February 2, 2006; revised April 27, 2006; accepted May 1, 2006; published May 5, 2006.

## LITERATURE CITED

**Allen E, Xie Z, Gustafson AM, Carrington JC** (2005) microRNA-directed phasing during trans-acting siRNA biogenesis in plants. Cell **121:** 207–221

**Ames BN** (1966) Assay of inorganic phosphate, total phosphate and phosphatases. Methods Enzymol **8:** 115–118

**Barber SA, Walker JM, Vasey EH** (1963) Mechanisms for the movement of plant nutrients from the soil and fertilizer to the plant root. J Agric Food Chem **11:** 204–207

**Bieleski RL** (1973) Phosphate pools, phosphate transport, and phosphate availability. Annu Rev Plant Physiol **24:** 225–252

**Burleigh SH, Harrison MJ** (1999) The down-regulation of Mt4-like genes by phosphate fertilization occurs systemically and involves phosphate translocation to the shoots. Plant Physiol **119:** 241–248

**Chen DL, Delatorre CA, Bakker A, Abel S** (2000) Conditional identification of phosphate-starvation-response mutants in *Arabidopsis thaliana.* Planta **211:** 13–22

**Chiou T-J, Aung K, Lin S-I, Wu C-C, Chiang S-F, Su C-l** (2006) Regulation of phosphate homeostasis by microRNA in Arabidopsis. Plant Cell **18:** 412–421

**Clough SJ, Bent AF** (1998) Floral dip: a simplified method for Agrobacterium-mediated transformation of *Arabidopsis thaliana.* Plant J **16:** 735–743

**Conti E, Izaurralde E** (2005) Nonsense-mediated mRNA decay: molecular insights and mechanistic variations across species. Curr Opin Cell Biol **17:** 316–325

**Curtis MD, Grossniklaus U** (2003) A gateway cloning vector set for high-throughput functional analysis of genes in planta. Plant Physiol **133:** 462–469

**Delhaize E, Randall PJ** (1995) Characterization of a phosphate-accumulator mutant of *Arabidopsis thaliana.* Plant Physiol **107:** 207–213

**Dong B, Rengel Z, Delhaize E** (1998) Uptake and translocation of phosphate by *pho2* mutant and wild-type seedlings of *Arabidopsis thaliana.* Planta **205:** 251–256

**Drew M, Saker L** (1984) Uptake and long-distance transport of phosphate, potassium and chloride in relation to internal ion concentrations in barley: evidence of non-allosteric regulation. Planta **160:** 500–507

**Dunlop J, Phung HT, Meeking R, White DWR** (1997) The kinetics associated with phosphate absorption by Arabidopsis and its regulation by phosphorus status. Aust J Plant Physiol **24:** 623–629

**Epstein E** (1976) Kinetics of ion transport and the carrier concept. *In* U Luttge, MG Pitman, eds, Transport in Plants, II. Part B; Tissues and Organs Encyclopedia of Plant Physiology, New Series, Vol 2B. Springer-Verlag, Berlin, pp 70–94

**Franco-Zorrilla JM, Gonzalez E, Bustos R, Linhares F, Leyva A, Paz-Ares J** (2004) The transcriptional control of plant responses to phosphate limitation. J Exp Bot **55:** 285–293

**Franco-Zorrilla JM, Martin AC, Leyva A, Paz-Ares J** (2005) Interaction between phosphate-starvation, sugar, and cytokinin signaling in Arabidopsis and the roles of cytokinin receptors CRE1/AHK4 and AHK3. Plant Physiol **138:** 847–857

**Franco-Zorrilla JM, Martin AC, Solano R, Rubio V, Leyva A, Paz-Ares J** (2002) Mutations at CRE1 impair cytokinin-induced repression of phosphate starvation responses in Arabidopsis. Plant J **32:** 353–360

**Fujii H, Chiou T-J, Lin S-I, Aung K, Zhu J-K** (2005) A miRNA involved in phosphate-starvation response in Arabidopsis. Curr Biol **15:** 2038–2043

**Furihata T, Suzuki M, Sakurai H** (1992) Kinetic characterization of two phosphate uptake systems with different affinities in suspension-cultured *Catharanthus roseus* protoplasts. Plant Cell Physiol **33:** 1151–1157

**González E, Solano R, Rubio V, Leyva A, Paz-Ares J** (2005) PHOSPHATE TRANSPORTER TRAFFIC FACILITATOR1 is a plant-specific SEC12-related protein that enables the endoplasmic reticulum exit of a high-affinity phosphate transporter in Arabidopsis. Plant Cell **17:** 3500–3512

**Hamburger D, Rezzonico E, MacDonald-Comber Petetot J, Somerville C, Poirier Y** (2002) Identification and characterization of the Arabidopsis PHO1 gene involved in phosphate loading to the xylem. Plant Cell **14:** 889–902

**Hammond JP, Bennett MJ, Bowen HC, Broadley MR, Eastwood DC, May ST, Rahn C, Swarup R, Woolaway KE, White PJ** (2003) Changes in gene expression in Arabidopsis shoots during phosphate starvation and the potential for developing smart plants. Plant Physiol **132:** 578–596

**Harrison MJ** (1999) Molecular and cellular aspects of the arbuscular mycorrhizal symbiosis. Annu Rev Plant Physiol Plant Mol Biol **50:** 361–389

**Hofstee BHJ** (1952) On the evaluation of the constants *V*m and *K*m in enzyme reactions. Science **116:** 329–331

**Holford ICR** (1997) Soil phosphorus: its measurement, and its uptake by plants. Aust J Soil Res **35:** 227–239

**Karimi M, De Meyer B, Hilson P** (2005) Modular cloning in plant cells. Trends Plant Sci **10:** 103–105

**Kraft E, Stone SL, Ma L, Su N, Gao Y, Lau O-S, Deng X-W, Callis J** (2005) Genome analysis and functional characterization of the E2 and RING-type E3 ligase ubiquitination enzymes of Arabidopsis. Plant Physiol **139:** 1597–1611

**Li M, Qin C, Welti R, Wang X** (2006) Double knockouts of phospholipases Dζ1 and Dζ2 in Arabidopsis affect root elongation during phosphate-limited growth but do not affect root hair patterning. Plant Physiol **140:** 761–770

**Lin S-I, Wang J-G, Poon S-Y, Su C-l, Wang S-S, Chiou T-J** (2005) Differential regulation of FLOWERING LOCUS C expression by vernalization in cabbage and Arabidopsis. Plant Physiol **137:** 1037–1048

**Lopez-Bucio J, Cruz-Ramirez A, Herrera-Estrella L** (2003) The role of nutrient availability in regulating root architecture. Curr Opin Plant Biol **6:** 280–287

**Lopez-Bucio J, Hernandez-Abreu E, Sanchez-Calderon L, Perez-Torres A, Rampey RA, Bartel B, Herrera-Estrella L** (2005) An auxin transport independent pathway is involved in phosphate stress-induced root architectural alterations in Arabidopsis. Identification of BIG as a mediator of auxin in pericycle cell activation. Plant Physiol **137:** 681–691

**Marschner H** (1995) Mineral Nutrition of Higher Plants. Academic Press, London

**McPharlin IR, Bieleski RL** (1987) Phosphate uptake by *Spirodela* and *Lemna* during early phosphorus deficiency. Aust J Plant Physiol **14:** 561–572

**Mimura T, Dietz K-J, Kaiser W, Schramm MJ, Kaiser G, Heber U** (1990) Phosphate transport across biomembranes and cytosolic phosphate homeostasis in barley leaves. Planta **180:** 139–146

**Misson J, Raghothama KG, Jain A, Jouhet J, Block MA, Bligny R, Ortet P, Creff A, Somerville S, Rolland N, et al** (2005) A genome-wide transcriptional analysis using Arabidopsis thaliana Affymetrix gene chips determined plant responses to phosphate deprivation. Proc Natl Acad Sci USA **102:** 11934–11939

**Misson J, Thibaud M-C, Bechtold N, Raghothama K, Nussaume L** (2004) Transcriptional regulation and functional properties of Arabidopsis Pht1;4, a high affinity transporter contributing greatly to phosphate uptake in phosphate deprived plants. Plant Mol Biol **55:** 727–741

**Miura K, Rus A, Sharkhuu A, Yokoi S, Karthikeyan AS, Raghothama KG, Baek D, Koo YD, Jin JB, Bressan RA, et al** (2005) The Arabidopsis SUMO E3 ligase SIZ1 controls phosphate deficiency responses. Proc Natl Acad Sci USA **102:** 7760–7765

**Mudge SR, Rae AL, Diatloff E, Smith FW** (2002) Expression analysis suggests novel roles for members of the Pht1 family of phosphate transporters in Arabidopsis. Plant J **31:** 341–353

**Nandi SK, Pant RC, Nissen P** (1987) Multiphasic uptake of phosphate by corn roots. Plant Cell Environ **10:** 463–474

**Narang RA, Bruene A, Altmann T** (2000) Analysis of phosphate acquisition efficiency in different Arabidopsis accessions. Plant Physiol **124:** 1786–1799

**Poirier Y, Bucher M** (2002) Phosphate transport and homeostasis in Arabidopsis. *In* CR Somerville, EM Meyerowitz, eds, The Arabidopsis Book. American Society of Plant Biologists, Rockville, MD, pp 1–35

**Poirier Y, Thoma S, Somerville C, Schiefelbein J** (1991) A mutant of Arabidopsis deficient in xylem loading of phosphate. Plant Physiol **97:** 1087–1093

**Raghothama KG** (1999) Phosphate acquisition. Annu Rev Plant Physiol Plant Mol Biol **50:** 665–693

**Rubio V, Linhares F, Solano R, Martin AC, Iglesias J, Leyva A, Paz-Ares J** (2001) A conserved MYB transcription factor involved in phosphate starvation signaling both in vascular plants and in unicellular algae. Genes Dev **15:** 2122–2133

**Sánchez-Cálderon L, Lopez-Bucio J, Chacon-Lopez A, Gutierrez-Ortega A, Hernandez-Abreu E, Herrera-Estrella L** (2006) Characterization of low phosphorus insensitive mutants reveals a crosstalk between low phosphorus-induced determinate root development and the activation of genes involved in the adaptation of Arabidopsis to phosphorus deficiency. Plant Physiol **140:** 879–889

**Schjørring JK, Jensén P** (1987) Phosphorus nutrient of barley, buckwheat and rape seedlings. I. Influence of seed-borne P and external P levels on growth, P content and $^{32}P/^{31}P$-fraction in shoots and roots. Physiol Plant **61:** 577–583

**Shimogawara K, Usuda H** (1995) Uptake of inorganic phosphate by suspension-cultured tobacco cells: kinetics and regulation by Pi starvation. Plant Cell Physiol **36:** 341–351

**Shin H, Shin H-S, Dewbre GR, Harrison MJ** (2004) Phosphate transport in Arabidopsis: Pht1;1 and Pht1;4 play a major role in phosphate acquisition from both low- and high-phosphate environments. Plant J **39:** 629–642

**Smith FW, Ealing PM, Dong B, Delhaize E** (1997) The cloning of two Arabidopsis genes belonging to a phosphate transporter family. Plant J **11:** 83–92

**Stadler R, Wright KM, Lauterbach C, Amon G, Gahrtz M, Feuerstein A, Oparka KJ, Sauer N** (2005) Expression of GFP-fusions in Arabidopsis companion cells reveals non-specific protein trafficking into sieve elements and identifies a novel post-phloem domain in roots. Plant J **41:** 319–331

**Sunkar R, Zhu J-K** (2004) Novel and stress-regulated microRNAs and other small RNAs from Arabidopsis. Plant Cell **16:** 2001–2019

**Ticconi CA, Abel S** (2004) Short on phosphate: plant surveillance and countermeasures. Trends Plant Sci **9:** 548–555

**Ticconi CA, Delatorre CA, Lahner B, Salt DE, Abel S** (2004) Arabidopsis *pdr2* reveals a phosphate-sensitive checkpoint in root development. Plant J **37:** 801–814

**Tomscha JL, Trull MC, Deikman J, Lynch JP, Guiltinan MJ** (2004) Phosphatase under-producer mutants have altered phosphorus relations. Plant Physiol **135:** 334–345

**Ullrich-Eberius CI, Novacky A, Bel AJE** (1984) Phosphate uptake in *Lemna gibba* G1: energetics and kinetics. Planta **161:** 46–52

**Versaw WK, Harrison MJ** (2002) A chloroplast phosphate transporter, PHT2;1, influences allocation of phosphate within the plant and phosphate-starvation responses. Plant Cell **14:** 1751–1766

**Wasaki J, Yonetani R, Kuroda S, Shinano T, Yazaki J, Fujii F, Shimbo K, Yamamoto K, Sakata K, Sasaki T, et al** (2003) Transcriptomic analysis of metabolic changes by phosphorus stress in rice plant roots. Plant Cell Environ **26:** 1515–1523

**Wu P, Ma L, Hou X, Wang M, Wu Y, Liu F, Deng XW** (2003) Phosphate starvation triggers distinct alterations of genome expression in Arabidopsis roots and leaves. Plant Physiol **132:** 1260–1271

**Zakhleniuk OV, Raines CA, Lloyd JC** (2001) *pho3*: a phosphorus-deficient mutant of *Arabidopsis thaliana* (L.) Heynh. Planta **212:** 529–534

**Zhu T, Lucas WJ, Rost TL** (1998) Directional cell-to-cell communication in the *Arabidopsis* root apical meristem I. An ultrastructural and functional analysis. Protoplasma **203:** 35–47